Evolution of thermal physiology alters predicted species distributions under climate change

Sara J.S. Wuitchik[1,†,*], Stephanie Mogensen[1], Tegan N. Barry[1], Antoine Paccard[2,‡], Heather A. Jamniczky[3], Rowan D.H. Barrett[2,§], and Sean M. Rogers[1,4,§]

[1]Department of Biological Sciences, University of Calgary, 2500 University Dr NW, Calgary, AB, T2N 1N4, CANADA

[2]Redpath Museum and Department of Biology, McGill University, 845 Sherbrooke St W, Montreal, QC, H3A 0G4, CANADA

[3]Department of Cell Biology & Anatomy, Cumming School of Medicine, University of Calgary, 3330 Hospital Dr NW, Calgary, T2N 4N1, CANADA

[4]Bamfield Marine Sciences Centre, 100 Pachena Rd, Bamfield, BC, V0R 1B0, CANADA

[§]equal co-senior authors

***Corresponding author: Sara J.S. Wuitchik**

E: sjswuit@g.harvard.edu

T: 857-292-9977

†Present affiliations: Informatics Group, Harvard University, 38 Oxford St, Cambridge, MA, 02138, USA & Department of Biology, Boston University, 5 Cummington Mall, Boston, MA, 02215, USA
‡Present affiliation: McGill University Genome Center, 740 Dr Penfield Avenue, Montreal, QC, H3A 1A5, Canada

Species distribution models (SDMs) are widely adopted to predict range shifts but can be unreliable under climate change scenarios[1] because they do not account for evolution. The thermal physiology of a species is a key determinant of range[2,3] but the impact of thermal trait evolution on SDMs has not been addressed. We identified a genetic basis for physiological traits that evolve in response to temperature change in threespine stickleback. Using these data, we created geographic range projections under two climate change scenarios where trait data was either static ('no evolution' model), allowed to evolve in agreement with published evolutionary rates for the trait ('evolution' model)[4], or allowed to evolve with the rate of evolution scaled in association with the variance that is explained by QTL ('PVE' model). Here, we show that incorporating these traits and their evolution into SDMs substantially altered the predicted ranges for a widespread panmictic marine population, with increases in area of over 7-fold. Evolution-informed SDMs should therefore improve the precision of forecasting range dynamics under climate change, thereby aiding in their application to management and the protection of biodiversity[5–7].

Temperature is a powerful driver of global biogeography and organism distributions frequently reflect temperature gradients in both aquatic and terrestrial habitats[8]. Many species adopt thermal strategies (such as thermoregulation or acclimation) that determine their thermal niche[9–11] and thermal traits can provide a target for directional selection if the environment changes to include temperatures outside the range encompassed by the thermal niche. Adaptation may thus permit species to persist at temperatures that would have previously led to extirpation[12,13]. Under moderate climate change scenarios, mean global oceanic temperature is predicted to increase in excess of 2°C by the end of the century[14], with more extreme changes predicted in localized regions[15]. Predicting species distribution patterns under climate change

therefore requires data for temperature-associated adaptive trait evolution, which can vary by species and population. While there have been recent steps to incorporate theoretical trait evolution into SDMs[3], to date, no model has used empirical estimates of evolutionary rate to inform predictions about future species distributions.

Due to widespread phenotypic variation[16], genomic resources[17], the availability of temperature-associated ecological and evolutionary trait data[4], and the ability to artificially breed multiple hybrid generations in a common garden lab environment, threespine stickleback fish (*Gasterosteus aculeatus*, Fig. 1a) are a useful vertebrate species for understanding the impact of adaptation on range dynamics under climate change. Here, we incorporate the specific capacity of marine populations to adapt their physiology to rapidly changing climate conditions to characterize how adaptive trait variation affects projections of species range distributions under climate change[18].

Results

We collected and reared wild marine and freshwater stickleback from two marine and two freshwater locations (Fig. 1b). These stickleback exhibited a wide thermal tolerance range bounded by a mean CTmin of 2.09 °C (+/- 1.13 °C SD) and a mean CTmax of 30.4 °C (+/- 2.64 °C SD)(Fig. 1c) and also tolerated a wide range of temperatures within which there was no observable stress response (5.0 – 25.0 °C). To determine if these measured thermal traits have a genetic basis and could therefore be subject to adaptive evolution, we raised hybrid marine-freshwater F1 (N=2) and F2 (N=4) families under common garden conditions and used these fish for genome-wide linkage map construction (Table S1) and quantitative trait loci (QTL) mapping. Using 25,001 high-quality single nucleotide variants generated from restriction site-associated

DNA (RAD) sequencing, we identified one significant QTL for each thermal tolerance trait (Fig. 2b) that explained a high percentage of trait variance (PVE; CTmin = 54%, CTmax = 64%).

We used these genetically based traits to inform the boundaries of three distinct environmental regions in species distribution models (SDMs) for marine stickleback based on varying levels of physiological performance: i) a 'normal behaviour' envelope with environmental temperatures associated with an absence of an observable behavioural stress response (5.0 to 25.0 °C), ii) a 'within physiological limits' envelope with environmental temperatures that fall within the range of the measured physiological limits (0.85 to 31.9 °C) , and iii) an 'outside of physiological limits' envelope with environmental temperatures that fall outside the measured physiological limits (below 0.85 and above 31.9 °C). Based on sea ice extent and bathymetry alone, our present-day correlative SDM suggests a marine range distribution for these stickleback from the southern Bering Sea to northern Washington state, and along the southeast Alaskan Panhandle (combined shaded area in Fig. 3a). When we include species-specific thermal trait data from the wild marine populations, nearly the entire range of suitable habitat was unaffected by thermal tolerance limits, with the exception of a slight restriction at the northern end of the range (Fig. 3a). However, when restricted to the Normal Behaviour area, the range becomes confined to the west of the northern tip of Kodiak Island (Fig. 3a), a limit coinciding with the northern-most known marine population in the Pacific Northwest genetic cluster[19].

We next generated SDMs based on predicted end-of-century environmental variables according to the Intergovernmental Panel on Climate Change (IPCC) representative concentration pathways (RCPs) 4.5 and 8.5 from the Fifth Assessment Report[14,20]. End-of-century IPCC predictions resulted in a substantial increase in the overall suitable habitat area for

stickleback, with a 2.25-fold or 1,338,219 km^2 increase (combined shaded area in Fig. 3b-e) in association with a reduction in sea ice concentration at the northern end of the range. When temperature increases as predicted by RCP 4.5 in the 'no evolution' model, there is a 5.86-fold (1,011,949 km^2) increase in the Normal Behaviour area within this newly suitable habitat (Fig. 3b) when compared to the current day model. Under RCP 8.5 in the 'no evolution' model, the entirety of suitable habitat area remains within tolerable limits (Fig. 3c), with a smaller proportion of the range falling outside of the Normal Behaviour area compared to RCP 4.5 (10.7%) 'no evolution' model.

Incorporating the evolution of CTmin into the SDMs ('evolution' model) results in a large increase in the proportion of suitable habitat that falls within the Normal Behaviour area. We allowed CTmin to evolve at a rate of 0.63 *haldanes*, which is equal to the rate observed for CTmin in marine stickleback[4] (there are currently no empirical estimates of evolutionary rate for CTmax). Under RCP 4.5, almost all (99.9%) of the suitable habitat range falls within the Normal Behaviour area (Fig. 3d), while under the RCP 8.5 'evolution' model, the entire range of suitable habitat is within the Normal Behaviour area (Fig. 3e). These represent a 7.45-fold increase (1,336,123 km^2) for RCP 4.5 and 7.46-fold increase (1,338,219 km^2) for RCP 8.5 in the Normal Behaviour area when compared to the current day SDM.

We next considered the effect of limiting the evolutionary rate of CTmin based on the observed genetic architecture of a single major effect locus ('PVE' model). Under the RCP 4.5 'PVE' model, we observed a 1.08-fold reduction in the Normal Behaviour area (109,120 km^2, Fig. S3) when compared to the 'evolution' model (Fig. 3d). Under RCP 8.5 projections with the 'PVE' model, we observed a 3,905 km^2 decrease in the Normal Behaviour area (Fig. S3) when compared to the 'evolution' model (Fig. 3e). This relatively small reduction in Normal

Behaviour area with adjusted PVE for the thermal traits under RCP 8.5 still results in a 1,334,314 km^2 increase in area compared to the current day SDM.

Discussion

We assessed the critical thermal minimum (CTmin) and maximum (CTmax) for threespine stickleback from wild marine and freshwater populations, as well as F1 and F2 families in order to determine the genetic basis underlying traits that will be important for population persistence under climate change. We incorporated the empirical ecological and evolutionary trait data from wild marine populations into mechanistic species distribution models under two climate change scenarios. We estimated the species distribution in the Pacific Northwest marine environment while these traits were held constant ('no evolution'), allowed CTmin to evolve in accordance with evolutionary rate estimates ('evolution'), and allowed CTmin to evolve at a constrained rate associated with the percent of trait variance explained by the single QTL we detected ('PVE'). The geographic ranges predicted for the end-of-century species distributions increased by over 7-fold (RCP 4.5: 1,336,123 km^2; RCP 8.5: 1,338,219 km^2) when CTmin was allowed to evolve, a substantial increase over the 'no evolution' model. Additionally, when CTmin evolution was constrained in the PVE model, there remained a ~6-fold increase (RCP 4.5: 1,227,002 km^2; RCP 8.5: 1,334,314 km^2) in the geographic range compared to current day. These differences in the predicted distributions underline the significance of incorporating empirical evolutionary data into SDMs[5,21,22], and in particular the need to consider behaviour in addition to physiology when predicting range shifts[23].

While the results presented here showcase the importance of creating more robust and informed SDMs, they also highlight a number of aspects that will benefit from additional consideration when interpreting these models. The existing estimate of CTmin evolution in

sticklebacks considered the change in phenotypic variation across generations[4], rather than evolution at underlying loci. As such, it is likely that some proportion of the observed phenotypic change was due to plastic responses. In our PVE model, we take a conservative approach by restricting phenotypic evolution of CTmin to only occur through heritable change via the locus shown to be associated with the trait. The efficiency of translating the selection acting on a trait into evolutionary response across generations can depend on the genetic architecture of the trait[24]. The large effect loci that we identified here are consistent with expectations from theory suggesting that prolonged bouts of adaptation with gene flow (as expected in this system[24–26]) should favour architectures characterized by fewer, larger effect, more tightly linked alleles[27–29]. However, it should be noted that the effects of the two QTL identified here are likely overestimated and other loci might have gone undetected (*sensu* the Beavis Effect[30]). The joint action of plastic effects and evolution at undetected loci might therefore result in range distributions that are more similar to those predicted in our 'evolution' models.

Climate change is leading to an increase in the frequency of extreme temperature events[14,31], including both extreme heat and extreme cold[32–34], which could drive selection on both CTmin and CTmax[13,35–37]. Our models reveal that the evolution of cold tolerance can have a significant impact on predicted range distributions despite most end-of-century climate change scenarios involving an overall warmer, not cooler world. This counterintuitive result occurs because climate change opens up newly available thermal niche space in waters north of the current day geographic range[20], and the evolution of CTmin extends this range expansion further still. Northward range expansion with climate change due to increasing habitat availability has also been documented in birds[38–41], plants[42], other fishes[43–45], and pest species (such as ticks[46–48] and mountain pine beetle[49,50]), as well as in large scale analyses of diverse taxa assessing the

159 'fingerprints' of climate change impacts[51,52]. However, it is likely that evolution of CTmax will
160 also play a role in responses to environmental change[53–55]. Although we have no empirical
161 estimates of CTmax evolution, it is interesting to explore how distributions would shift if we
162 observed the same rate of evolution in this trait as in CTmin. Using the same rate of haldanes and
163 incorporating our observed PVE for the locus associated with CTmax, we find that geographic
164 ranges predicted for the end-of-century species distributions also increased by over 7-fold (RCP
165 4.5: 1,227,002 km^2 increase; RCP 8.5: 1,334,314 km^2 increase; Fig. S4). Further investigations to
166 test the empirical rate of evolution of thermal behaviour, physiology and the molecular
167 underpinnings of these key traits would be well served by assessing additional samples along the
168 latitudinal gradient inhabited by stickleback to gain a more detailed understanding of these
169 temperature-associated traits over a wider environmental range.

170 Collectively, the inclusion of thermal traits and their evolution alters the projected ranges
171 of threespine stickleback, with a substantial increase in the predicted area that the species will
172 occupy under climate change forecasts. Many traits are evolving in response to climate change[56–
173 59] and SDMs that do not take trait data (and trait evolution) into account could provide inaccurate
174 predictions about future species distributions under climate change[3] - an issue of particular
175 concern for species at risk and pest species undergoing range expansion[60–62]. Our results provide
176 a framework for addressing this problem, which will have critical implications for the application
177 of these models in policy and resource management, and the protection of biodiversity in a
178 changing climate.

Materials and Methods

Sample collection and husbandry

We collected adult *Gasterosteus aculeatus* (Fig. 1a) from two marine populations (Bamfield, M1, 48°49'12.69"N 125° 8'57.90"W; Garden Bay Lagoon, M2, 49°37'52.84"N 124° 1'49.26"W) and two freshwater populations (Hotel Lake, FW1, 49°38'26.94"N 124° 3'0.69"W; Klein Lake, FW2, 49°43'32.47"N 123°58'7.83"W) in southwestern British Columbia (Fig. 1b). Individuals were maintained in a flow-through system and photoperiod that mimicked the source populations during collection periods before transport. We transported the fish to our aquatics facility in the Life and Environmental Sciences Animal Resources Centre at the University of Calgary, where we separated the fish into population-specific 113 L glass aquaria at a density of approximately 20 fish per aquarium. We acclimated marine individuals to freshwater salinity over one week and maintained fish in a common environment (salinity of 4-6 ppt, water temperature of 15 ± 2 °C, and a photoperiod of 16L:8D). Individuals were allowed to acclimate for at least 2 weeks before experiments (1 week for stress reduction post-transfer, 1 week for common garden environment acclimation and salinity ramp). Each common garden aquarium was on a closed system with individual filters, air stones, and water supply. We fed all adult fish *ad libitum* once per day with thawed bloodworms (Hikari Bio-Pure Frozen Bloodworms). All collections and transfers were approved by the Department of Fisheries and Oceans (marine collections and transfers), the Ministry of Forests, Lands, and Natural Resource Operations (freshwater collections), and the Huu-ay-aht First Nations (marine collections).

Crossing design for marine and freshwater F1 families

We collected eggs from females and fertilized the eggs with extracted testes from euthanized males. We transferred the fertilized egg mass to a mesh-bottomed egg incubator

suspended in a 37 L aquarium for hatching. Each hatching aquarium was maintained with a single air stone and a filter. Once hatched, we reared the larval fish in 37 L hatching aquaria until they reached a total length (TL) of approximately 1 cm, after which we split the families into family-specific 113 L aquaria to maintain suitable densities. We fed the larval fish *ad libitum* twice daily with live *Artemia spp.* nauplii, and then gradually transitioned the diet to chopped, thawed bloodworms (Hikari Bio-Pure Frozen Bloodworms) *ad libitum* once daily as they reached approximately 2 cm TL. The F1 families were maintained in a common garden environment identical to that of the F0 populations. We produced one F1 family for each population (M1_F1, M2_F2, FW1_F1, and FW2_F1).

Crossing design for hybrid mapping families

To generate genetically heterogeneous marine-freshwater F1 families from wild F0 parents, we collected eggs from marine females and fertilized the eggs with extracted testes from euthanized freshwater males. Egg masses were hatched, and juveniles were reared, as detailed above. Overall, we produced one F1 family of M1xFW1 hybrids (hereafter referred to as H1_F1) and three F1 families of M1xFW2 hybrids (hereafter referred to as H2_F1). The hybrid F1 families were maintained in a common garden environment identical to that of the F0 populations. To generate F2 families for linkage map construction, we crossed individuals from the same F1 family with the same methodology used to generate the F1 families. Overall, we produced one F2 family of H1xH1 hybrids (referred to as H1_F2) and three families of H2xH2 hybrids (referred to as H2_F2_1, H2_F2_2, and H2_F2_3). All F2 individuals were raised as described above in a common garden environment identical to that of the F0 and F1 individuals to ensure consistent history and use for QTL mapping.

Thermal tolerance experiments

To assess the lower and upper limits of physiological thermal tolerance, we conducted standard critical thermal minimum (CTmin) and maximum (CTmax) experiments on adult fish[4,63,64]. At these sublethal limits, the fish experiences a loss of equilibrium (LOE) at which they lose the ability to escape conditions that would ultimately lead to their death in nature[65]. Our experimental tank held 1000 mL glass beakers aerated individually to prevent thermal stratification. Before each experiment, individuals were fasted for 24 hours. After a 15-minute acclimation to the experimental apparatus in the individual beakers, we cooled or heated the water (for CTmin or CTmax, respectively) at a rate of approximately 0.33 °C min^{-1}. We assessed wild F0 individuals (n_{M1} = 32, n_{M2} = 14, n_{FW1} = 15, n_{FW2} = 16, N = 77; Fig. 1c) and lab raised F1 (n_{M1_F1} = 13, n_{M2_F1} = 15, n_{FW1_F1} = 15, n_{FW2_F1} = 15, N = 58; Fig. S1) and F2 individuals (n_{H1_F2} = 28, $n_{H2\_F2\_1}$ = 36, $n_{H2\_F2\_2}$ = 21, $n_{H2\_F2\_3}$ = 17, N = 102; Fig. S2). All individuals were assessed for CTmin, allowed to recover for at least three days, then assessed for CTmax to keep thermal stress history consistent. The onset of erratic behaviours associated with a behavioural stress response occurred below 5.0 °C and above 25.0 °C during CTmin and CTmax experiments, respectively. Normal behaviour was observed between 5.0 °C and 25.0 °C, whereas outside of those temperatures, individuals gradually exhibited more extreme stress responses (*e.g.,* increased gilling rate, erratic movement, muscle spasms, listing, as outlined by the Canadian Council of Animal Care guidelines) until reaching LOE and the inability of an individual to right itself (the experimental endpoint)[4,63,64]. At the time of data collection for thermal trait experiments, all individuals were adults.

Isolation and characterization of single nucleotide polymorphisms (SNPs)

Genomic DNA was extracted from caudal fin tissue using a phenol-chloroform-based protocol. We digested tissues overnight in digestion buffer and proteinase K at 55 °C, then performed multiple phenol-chloroform and ethanol washes to isolate the DNA. We assessed the quantity of the extracted DNA using the Quant-iT PicoGreen dsDNA assay kit (ThermoFisher Scientific, Waltham, MA, USA) and Synergy HT plate reader with the Gen5 associated software (BioTek, Winooski, VT, USA). We prepared restriction site-associated DNA (RAD) libraries(Peterson et al. 2012) using *MluCl* and *NlaIII* restriction (New England Biolabs, Ipswich, MA, USA), ligation of individual barcodes, and pooling of 48 individuals per library at equimolar concentrations. We performed a final PCR to amplify DNA and add library-specific indices to allow for pooling of multiple libraries. We sequenced three libraries at McGill University and Génome Québec Innovation Center on one lane of Illumina HiSeq 4000 (Illumina Inc., San Diego, CA, USA).

Assembly of genetic linkage map

After barcode demultiplexing and filtering out low quality reads in STACKS[66], we removed PCR duplicates from the raw sequences and aligned to the *G. aculeatus* reference genome[17] using the Burrows-Wheeler transform[67]. Individual libraries were concatenated and filtered[68] using *vcftools* v3.0[69] and then split into chromosome-specific VCF files to assemble the linkage maps chromosome by chromosome. We assigned markers to a linkage group with an initial LOD score of 3 after filtering out markers that showed high levels of segregation distortion and missing observations (> 20% missing data) in Lep-MAP3[70]. Unassigned markers were subsequently added to the existing linkage group at a LOD score of 3 and a size limit of 5 markers per linkage group. We ordered the markers using a minimum posterior value of 0.001

and collapsed multiple markers when the probability difference between markers was < 0.01[70]. The final linkage map was subset for use in R[71] with a custom Python script to visualize the linkage map and to generate a list of informative SNPs to use in subsequent analyses with the *qtl* v1.44-9[72] and *qtlTools* v1.2.0[73] packages. Linkage maps were visualized using *LinkageMapView*[74] in R[71]. The final linkage maps were similar across families in number of markers, length, and spacing between markers, though the H1_F2 map did have a higher density of markers (Table S1).

Quantitative trait loci (QTL) mapping

We analysed families separately with the same methodology to assess the presence of QTL associated with the thermal traits. We calculated conditional genotype probabilities using hidden Markov model technology and simulated genotypes based on the observed marker data (allowing for possible genotyping errors at a level of 0.0001 using a Kosambi mapping function with a fixed step width) prior to running genome scans with a single QTL model[75,76]. We determined the logarithm of the odds (LOD) score significance thresholds for each trait through permutation tests for each family (100,000 permutations) (Fig. 2a). We pulled significant QTL above the genome-wide significance threshold ($\alpha = 0.05$[77]), calculated confidence intervals of QTL location based on nearby markers, and estimated the percent variance explained by each QTL peak marker. We identified two QTL on linkage group 4 (which corresponds to chromosome 4 of the BROAD assembly[17]) associated with CTmin and CTmax (Fig. 2b).

Environmental variables and species distribution models (SDMs)

We compiled environmental data widely used in the construction of SDMs to estimate suitable habitat in both present day and end-of-century forecasts[78], including bathymetry, sea ice extent and concentration, salinity, and sea surface temperature. We used 2014 data as our

baseline year to match the forecasting baseline of the Fifth Assessment Report[14]. We assumed a suitable habitat range for this species in the Pacific Northwest to consist of coastal areas (where the water depth is less than 200 m) where sea ice is never present (*i.e.,* no sea ice at the maximum extent). The salinity tolerance for *G. aculeatus* is very wide[79,80] and salinity was not limiting in any of the habitat[81], therefore salinity was not included in the final present day or forecasted models. We obtained bathymetry data from the General Bathymetric Chart of the Oceans (GEBCO) of the British Oceanographic Data Centre[82], and maximum sea ice extent data from the Multisensory Analyzed Sea Ice Extent – Northern Hemisphere (MASIE-NH) product[83]. We obtained maximum and minimum daily mean sea surface temperature (SST)[84]. Sea surface temperature was used as a proxy for water temperature. Stickleback thermal trait data were used to set the limits of the distribution within the possible area delineated by sea ice free water of a suitable depth (Table S2). The thermal trait measurements were all based on our experimental findings reported here.

In the end-of-century forecast for suitable habitat, we assumed bathymetry to be consistent with the modern scenario. However, the Arctic Ocean is predicted to be predominantly free of sea ice in the summer by the end of the century[85], with significant end-of-century reductions in winter/spring sea ice concentration (reduced to a concentration of 0.1 at the Seward Peninsula[85]), so we conservatively set the maximum northern extent of the suitable habitat to be 65°35' N, which corresponds to the western tip of the Seward Peninsula (near Wales, AK). The extent of sea ice was kept consistent between scenarios to control for area in calculations of range expansion. The water temperatures were increased based on projections for large marine ecosystems of Northern Oceans from global climate models[14,20]. Maps were created in R[71] using the packages *raster* v. 3.3-13[86] and *rgeos* v. 0.5-3[87].

We incorporated the experimental data from the critical thermal minimum and maximum trials on the wild marine populations (Fig. 1c) to understand how trait inclusion may affect range projections under climate change. These trait-defined envelopes were overlain on the suitable habitat background to delineate projected presence based on thermal traits in both current day and IPCC predicted RCPs 4.5 and 8.5. The trait values were kept constant (*i.e.,* not changed) in the 'no evolution' projections, but in the 'evolution' projections, we allowed CTmin to evolve an improvement of 2.5 °C (*i.e.,* 2.5 °C lower than CTmin boundary in the 'no evolution' projection) by the end of the century based on a rate of 0.63 *haldanes* from a selection experiment previously conducted on populations from this same genetic cluster[4]. The 'evolution' model assumes whole-organism tolerance evolution with selection acting on 100% of the loci affecting CTmin evolution. Therefore, to account for the observed genetic architecture of a single, large effect locus associated with CTmin, we next considered a 'PVE' model, where CTmin was allowed to evolve to only 54% of the total estimated trait value from the 'evolution' model (*i.e.,* 2.5 °C * 0.54). However, a notable restriction in the evolution of CTmin for both models ('evolution' and 'PVE') was a hard boundary drawn at 0 °C under the assumption that population persistence in a sub-zero environment would require many additional adaptations alongside CTmin improvement (*e.g.,* extreme adaptations observed in Antarctic notothenioid fishes[88–90]).

To quantify the differences in estimated suitable habitat under current day and end-of-century conditions, we compared areas for each warming scenario to the equivalent scenario under current conditions. Similarly, to compare the differences in evolutionary scenarios, the area of each end-of-century evolutionary trajectory was compared to either the contrasting RCP projection or adjusted PVE projection. For these comparisons, we used North Pole Lambert

337 azimuthal equal area projection for all maps, and georeferenced to known landmarks in ArcGIS
338 v10.8[91] to calculate area from the maps generate in R[71] (conversion ratio of 7873.42).

339 The datasets generated and analysed during the current study are available from the
340 corresponding author upon reasonable request. The annotated code, including all parameter
341 thresholds, for the above QTL analyses and SDM construction is publicly available on Github
342 (github.com/sjswuitchik/gasAcu_qtl_sdm).

343

344 **References**

345 1. Kearney, M. R., Wintle, B. A. & Porter, W. P. Correlative and mechanistic models of
346 species distribution provide congruent forecasts under climate change. *Conserv. Lett.* **3**,
347 203–213 (2010).

348 2. Kearney, M. & Porter, W. Mechanistic niche modelling: Combining physiological and
349 spatial data to predict species' ranges. *Ecol. Lett.* **12**, 334–350 (2009).

350 3. Bush, A. *et al.* Incorporating evolutionary adaptation in species distribution modelling
351 reduces projected vulnerability to climate change. *Ecol. Lett.* **19**, 1468–1478 (2016).

352 4. Barrett, R. D. H. *et al.* Rapid evolution of cold tolerance in stickleback. *Proc. R. Soc. B*
353 **278**, 233–238 (2011).

354 5. Evans, T. G., Diamond, S. E. & Kelly, M. W. Mechanistic species distribution modelling
355 as a link between physiology and conservation. *Conserv. Physiol.* **3**, 1–16 (2015).

356 6. Pearce, J. & Lindenmayer, D. Bioclimatic analysis to enhance reintroduction biology of
357 the endangered helmeted honeyeater (Lichenostomus melanops cassidix) in southeastern

Australia. *Restor. Ecol.* **6**, 238–243 (1998).

7. Araújo, M. B., Cabeza, M., Thuiller, W., Hannah, L. & Williams, P. H. Would climate change drive species out of reserves? An assessment of existing reserve-selection methods. *Glob. Chang. Biol.* **10**, 1618–1626 (2004).

8. Hochachka, P. W. & Somero, G. N. Mechanism and process in physiological evolution. *Biochem. Adapt.* **480**, (2002).

9. Huey, R. B. & Slatkin, M. Costs and benefits of lizard thermoregulation. *Q. Rev. Biol.* **51**, 363–384 (1976).

10. Coutant, C. C. Thermal preference: when does an asset become a liability? *Environ. Biol. Fishes* **18**, 161–172 (1987).

11. Huey, R. B. & Kingsolver, J. G. Evolution of thermal sensitivity of ectotherm performance. *Trends Ecol. Evol.* **4**, 131–135 (1989).

12. Sexton, J. P., McIntyre, P. J., Angert, A. L. & Rice, K. J. Evolution and Ecology of Species Range Limits. *Annu. Rev. Ecol. Evol. Syst.* **40**, 415–436 (2009).

13. Hoffman, A. & Sgrò, C. Climate change and evolutionary adaptation. *Nature* **470**, 479–485 (2011).

14. IPCC. *Climate Change 2014: Synthesis Report*. *Fifth Assessment Report of the Intergovernmental Panel on Climate Change* (2014). doi:10.1016/S0022-0248(00)00575-3

15. Eyer, P. A., Blumenfeld, A. J. & Vargo, E. L. Sexually antagonistic selection promotes

genetic divergence between males and females in an ant. *Proc. Natl. Acad. Sci. U. S. A.* **116**, 24157–24163 (2019).

16. Hendry, A. P., Peichel, C. L., Matthews, B., Boughman, J. W. & Nosil, P. Stickleback research: The now and the next. *Evol. Ecol. Res.* **15**, 111–141 (2013).

17. Jones, F. C. *et al.* The genomic basis of adaptive evolution in threespine sticklebacks. *Nature* **484**, 55–61 (2012).

18. Barrett, R. D. H. & Hendry, A. P. Evolutionary rescue under environmental change. in *Behavioural responses to a changing world: mechanisms and consequences* 216–233 (Oxford University Press Oxford, UK, 2012).

19. Morris, M. R. J., Bowles, E., Allen, B. E., Jamniczky, H. A. & Rogers, S. M. Contemporary ancestor? Adaptive divergence from standing genetic variation in Pacific marine threespine stickleback. *BMC Evol. Biol.* **18**, 1–21 (2018).

20. Alexander, M. A. *et al.* Projected sea surface temperatures over the 21st century: Changes in the mean, variability and extremes for large marine ecosystem regions of Northern Oceans. *Elementa* **6**, (2018).

21. Buckley, L. *et al.* Can mechanism inform species' distribution models? *Ecol. Lett.* **13**, 1041–1054 (2010).

22. Lyon, N. J., Debinski, D. M. & Rangwala, I. Evaluating the Utility of Species Distribution Models in Informing Climate Change-Resilient Grassland Restoration Strategy. *Front. Ecol. Evol.* **7**, 1–8 (2019).

398 23. Sunday, J. M., Bates, A. E. & Dulvy, N. K. Thermal tolerance and the global
399 redistribution of animals. *Nat. Clim. Chang.* **2**, 686–690 (2012).

400 24. Rogers, S. M. *et al.* Genetic Signature of Adaptive Peak Shift in Threespine Stickleback.
401 *Evolution (N. Y).* 2439–2451 (2012). doi:10.5061/dryad.6jj614kh

402 25. Schluter, D., Marchinko, K. B., Barrett, R. D. H. & Rogers, S. M. Natural selection and
403 the genetics of adaptation in threespine stickleback. *Philos. Trans. R. Soc. B Biol. Sci.* **365**,
404 2479–2486 (2010).

405 26. Jones, F. C. *et al.* A genome-wide SNP genotyping array reveals patterns of global and
406 repeated species-pair divergence in sticklebacks. *Curr. Biol.* **22**, 83–90 (2012).

407 27. Yeaman, S. & Otto, S. P. Establishment and maintenance of adaptive genetic divergence
408 under migration, selection, and drift. *Evolution (N. Y).* **65**, 2123–2129 (2011).

409 28. Yeaman, S. & Whitlock, M. C. The genetic architecture of adaptation under migration-
410 selection balance. *Evolution (N. Y).* **65**, 1897–1911 (2011).

411 29. Via, S., Conte, G., Mason-Foley, C. & Mills, K. Localizing FST outliers on a QTL map
412 reveals evidence for large genomic regions of reduced gene exchange during speciation-
413 with-gene-flow. *Mol. Ecol.* **21**, 5546–5560 (2012).

414 30. Beavis, W. The power and deceit of QTL experiments: lessons from comparative QTL
415 studies. in *49th Annual Corn & Sorghum Research Conference* 250–266 (1994).

416 31. Stott, P. How climate change affects extreme weather events. *Science (80-.).* **352**, 1517–
417 1518 (2016).

418 32. Herring, S., Hoerling, M., Kossing, J., Peterson, T. & Stott, P. Explaining extreme events
419 of 2014 from a climate perspective. **96**, 1–180 (2015).

420 33. Herring, S. C. *et al.* Explaining extreme events of 2016 from a climate perspective. *Bull.*
421 *Am. Meteorol. Soc.* **99**, S1–S157 (2018).

422 34. Herring, S. C., Christidis, N., Hoell, A., Hoerling, M. P. & Stott, P. Explaining extreme
423 events of 2018 from a climate perspective. *Bull. Am. Meteorol. Soc.* **101**, 1–146 (2020).

424 35. Kingsolver, J. G. *et al.* Complex life cycles and the responses of insects to climate change.
425 *Integr. Comp. Biol.* **51**, 719–732 (2011).

426 36. Denny, M. W. & Dowd, W. W. Biophysics, environmental stochasticity, and the evolution
427 of thermal safety margins in intertidal limpets. *J. Exp. Biol.* **215**, 934–947 (2012).

428 37. Buckley, L. B. & Huey, R. B. How extreme temperatures impact organisms and the
429 evolution of their thermal tolerance. *Integr. Comp. Biol.* **56**, 98–109 (2016).

430 38. Tingley, M. W., Monahan, W. B., Beissinger, S. R. & Moritz, C. Birds track their
431 Grinnellian niche through a century of climate change. *Proc. Natl. Acad. Sci. U. S. A.* **106**,
432 19637–19643 (2009).

433 39. Melles, S. J., Fortin, M. J., Lindsay, K. & Badzinski, D. Expanding northward: Influence
434 of climate change, forest connectivity, and population processes on a threatened species'
435 range shift. *Glob. Chang. Biol.* **17**, 17–31 (2011).

436 40. Tombre, I. M., Oudman, T., Shimmings, P., Griffin, L. & Prop, J. Northward range
437 expansion in spring-staging barnacle geese is a response to climate change and population

growth, mediated by individual experience. *Glob. Chang. Biol.* **25**, 3680–3693 (2019).

41. Rushing, C. S., Andrew Royle, J., Ziolkowski, D. J. & Pardieck, K. L. Migratory behavior and winter geography drive differential range shifts of eastern birds in response to recent climate change. *Proc. Natl. Acad. Sci. U. S. A.* **117**, 12897–12903 (2020).

42. D'Andrea, L. *et al.* Climate change, anthropogenic disturbance and the northward range expansion of Lactuca serriola (Asteraceae). *J. Biogeogr.* **36**, 1573–1587 (2009).

43. Fossheim, M. *et al.* Recent warming leads to a rapid borealization of fish communities in the Arctic. *Nat. Clim. Chang.* **5**, 673–677 (2015).

44. Yapıcı, S., Bilge, G. & Filiz, H. Northwards range expansion of Sparisoma cretense (Linnaeus, 1758) in the Turkish Aegean Sea. *J. Aquac. Eng. Fish. Res.* 201–207 (2016). doi:10.3153/jaefr16022

45. Spies, I. *et al.* Genetic evidence of a northward range expansion in the eastern Bering Sea stock of Pacific cod. *Evol. Appl.* **13**, 362–375 (2020).

46. Ogden, N. H. *et al.* Climate change and the potential for range expansion of the Lyme disease vector Ixodes scapularis in Canada. *Int. J. Parasitol.* **36**, 63–70 (2006).

47. Clow, K. M. *et al.* Northward range expansion of Ixodes scapularis evident over a short timescale in Ontario, Canada. *PLoS One* **12**, 1–15 (2017).

48. Sagurova, I. *et al.* Predicted northward expansion of the geographic range of the tick vector amblyomma americanum in North America under future climate conditions. *Environ. Health Perspect.* **127**, 1–14 (2019).

458 49. Kurz, W. A. *et al.* Mountain pine beetle and forest carbon feedback to climate change.
459 *Nature* **452**, 987–990 (2008).

460 50. Sambaraju, K. R., Carroll, A. L. & Aukema, B. H. Multiyear weather anomalies
461 associated with range shifts by the mountain pine beetle preceding large epidemics. *For.*
462 *Ecol. Manage.* **438**, 86–95 (2019).

463 51. Parmesan, C. & Yohe, G. A globally coherent fingerprint of climate change impacts
464 across natural systems. **421**, 37–42 (2003).

465 52. Platts, P. J. *et al.* Habitat availability explains variation in climate-driven range shifts
466 across multiple taxonomic groups. *Sci. Rep.* **9**, 1–10 (2019).

467 53. Geerts, A. N. *et al.* Rapid evolution of thermal tolerance in the water flea Daphnia. *Nat.*
468 *Clim. Chang.* **5**, 665–668 (2015).

469 54. Bozinovic, F., Medina, N. R., Alruiz, J. M., Cavieres, G. & Sabat, P. Thermal tolerance
470 and survival responses to scenarios of experimental climatic change: changing thermal
471 variability reduces the heat and cold tolerance in a fly. *J. Comp. Physiol. B Biochem. Syst.*
472 *Environ. Physiol.* **186**, 581–587 (2016).

473 55. Cuenca Cambronero, M., Beasley, J., Kissane, S. & Orsini, L. Evolution of thermal
474 tolerance in multifarious environments. *Mol. Ecol.* **27**, 4529–4541 (2018).

475 56. Eliason, E. J. *et al.* Differences in thermal tolerance among sockeye salmon populations.
476 *Science (80-.).* **332**, 109–112 (2011).

477 57. Hovel, R. A., Carlson, S. M. & Quinn, T. P. Climate change alters the reproductive

phenology and investment of a lacustrine fish, the three-spine stickleback. *Glob. Chang. Biol.* 1–13 (2016). doi:10.1111/gcb.13531

58. Gómez-Ruiz, E. P. & Lacher, T. E. Climate change, range shifts, and the disruption of a pollinator-plant complex. *Sci. Rep.* **9**, 1–10 (2019).

59. Horton, K. G. *et al.* Phenology of nocturnal avian migration has shifted at the continental scale. *Nat. Clim. Chang.* **10**, 63–68 (2020).

60. Cullingham, C. I. *et al.* Mountain pine beetle host-range expansion threatens the boreal forest. *Mol. Ecol.* **20**, 2157–2171 (2011).

61. McLeod, D. J., Hallegraeff, G. M., Hosie, G. W. & Richardson, A. J. Climate-driven range expansion of the red-tide dinoflagellate Noctiluca scintillans into the Southern Ocean. *J. Plankton Res.* **34**, 332–337 (2012).

62. Bebber, D. P. Range-Expanding Pests and Pathogens in a Warming World. *Annu. Rev. Phytopathol.* **53**, 335–356 (2015).

63. Hutchison, V. H. Comparative Biology Critical Thermal Maxima in Salamanders. *Physiol. Zool.* **34**, 92–125 (1961).

64. Fangue, N. A., Hofmeister, M. & Schulte, P. M. Intraspecific variation in thermal tolerance and heat shock protein gene expression in common killifish, Fundulus heteroclitus. *J. Exp. Biol.* **209**, 2859–2872 (2006).

65. Beitinger, T., Bennett, W. & McCauley, R. Temperature tolerances of North American freshwater fishes exposed to dynamic changes in temperature. *Environ. Biol. Fishes* **58**,

237–275 (2000).

66. Catchen, J., Hohenlohe, P. A., Bassham, S., Amores, A. & Cresko, W. A. Stacks: An analysis tool set for population genomics. *Mol. Ecol.* **22**, 3124–3140 (2013).

67. Li, H. & Durbin, R. Fast and accurate long-read alignment with Burrows-Wheeler transform. *Bioinformatics* **26**, 589–595 (2010).

68. Puritz, J. B., Hollenbeck, C. M. & Gold, J. R. *dDocent* : a RADseq, variant-calling pipeline designed for population genomics of non-model organisms. *PeerJ* **2**, e431 (2014).

69. Danecek, P. *et al.* The variant call format and VCFtools. *Bioinformatics* **27**, 2156–2158 (2011).

70. Rastas, P. Lep-MAP3: Robust linkage mapping even for low-coverage whole genome sequencing data. *Bioinformatics* **33**, 3726–3732 (2017).

71. R Core Team. R: A language and environment for statistical computing. (2019).

72. Broman, K. W., Wu, H., Sen, Ś. & Churchill, G. A. R/qtl: QTL mapping in experimental crosses. *Bioinformatics* **19**, 889–890 (2003).

73. Lovell, J. qtlTools. (2019).

74. Ouellette, L. A., Reid, R. W., Blanchard, S. G. & Brouwer, C. R. LinkageMapView-rendering high-resolution linkage and QTL maps. *Bioinformatics* **34**, 306–307 (2018).

75. Broman, K. W. & Sen, S. *A Guide to QTL Mapping with R/qtl*. **46**, (Springer, 2009).

76. Arends, D., Prins, P., Broman, K. W. & Jansen, R. C. *Tutorial-Multiple-QTL Mapping*

(MQM) Analysis for R/qtl. *http://www.rqtl.org/tutorials/MQM-tour.pdf* (2014).

77. Greenwood, A. K. *et al.* The genetic basis of divergent pigment patterns in juvenile threespine sticklebacks. *Heredity (Edinb).* **107**, 155–166 (2011).

78. Wiens, J., Stralberg, D., Jongsomjit, D., Howell, C. & Snyder, M. Niches, models, and climate change: Assessing the assumptions and uncertainties. *Proc. Natl. Acad. Sci.* **106**, 19729–19736 (2009).

79. Bayly, I. A. E. Salinity Tolerance and Osmotic Behavior of Animals in Athalassic Saline and Marine Hypersaline Waters. *Annu. Rev. Ecol. Syst.* **3**, 233–268 (2003).

80. Divino, J. N. *et al.* Osmoregulatory physiology and rapid evolution of salinity tolerance in threespine stickleback recently introduced to fresh water. *Evol. Ecol. Res.* **17**, 179–201 (2016).

81. Zweng, M. M. *et al. World Ocean Atlas 2013, Volume 2: Salinity*. *NOAA Atlas NESDIS 74* **2**, (2013).

82. Weatherall, P. *et al.* A new digital bathymetric model of the world's oceans. *Earth Sp. Sci.* **2**, 331–345 (2015).

83. Fetterer, F., Savoie, M., Helfrich, S. & Clemene-Colon, P. U.S. National Ice Center and National Snow and Ice Data Center. *Multisensor Analyzed Sea Ice Extent - Northern Hemisphere (MASIE-NH)* (2010). doi:https://doi.org/10.7265/N5GT5K3K.

84. Reynolds, R. *et al.* Daily High-Resolution-Blended Analyses for Sea Surface Temperature. *J. Clim.* **20**, 5473–5496 (2007).

537 85. Johannessen, O. *et al.* Arctic climate change: observed and modelled temperature and sea-
538 ice variability. *Tellus A Dyn. Meteorol. Oceanogr.* **56**, 328–341 (2004).

539 86. Hijmans, R. J. *et al.* raster: Geographic data analysis and modelling. (2020).

540 87. Roger, A., Stuetz, R., Ove, K., Giraudoux, P. & Santilli, S. rgeos: Interface to geometry
541 engine - open. (2020).

542 88. Detrich, H. W., Parker, S. K., Williams, J., Nogales, E. & Downing, K. H. Cold adaptation
543 of microtubule assembly and dynamics. Structural interpretation of primary sequence
544 changes present in the α- and β-tubulins of antarctic fishes. *J. Biol. Chem.* **275**, 37038–
545 37047 (2000).

546 89. Cheng, C. H. C. & Detrich, H. W. Molecular ecophysiology of Antarctic notothenioid
547 fishes. *Philos. Trans. R. Soc. B Biol. Sci.* **362**, 2215–2232 (2007).

548 90. Shin, S. C. hu. *et al.* The genome sequence of the Antarctic bullhead notothen reveals
549 evolutionary adaptations to a cold environment. *Genome Biol.* **15**, 468 (2014).

550 91. Environmental Systems Research Institute. ArcGIS Desktop: Release 10.8. (2017).

551 Acknowledgments

552 The authors acknowledge that the species collections took place on Huu-ay-aht and Sechelt First
553 Nations traditional territories and are grateful for the opportunity to conduct their research in
554 protected and sacred areas. We would like to thank the Bamfield Marine Sciences Centre for the
555 resources required to conduct this research, Sam Owens for the photo in Figure 1a, Peter Peller
556 for creating Figure 1b, as well as Daniel Wuitchik, Sam Yeaman, Jennifer Sunday, and Patrick
557 Nosil for feedback on the manuscript.

558 **Author Contributions**

559 This study was designed by SJSW, RDHB, and SMR; fish husbandry and breeding by SJSW and

560 TNB; experimental data collection by SJSW; DNA sequencing and initial processing by AP;

561 bioinformatic and QTL analyses by SJSW; species distribution modelling by SJSW and SM; the

562 manuscript was written by SJSW, RDHB, and SMR, with input from authors; the study was

563 funded by HAJ, RDHB, and SMR.

564

565 Competing Interests: The authors declare no competing interests.

566

567

Figures and Tables

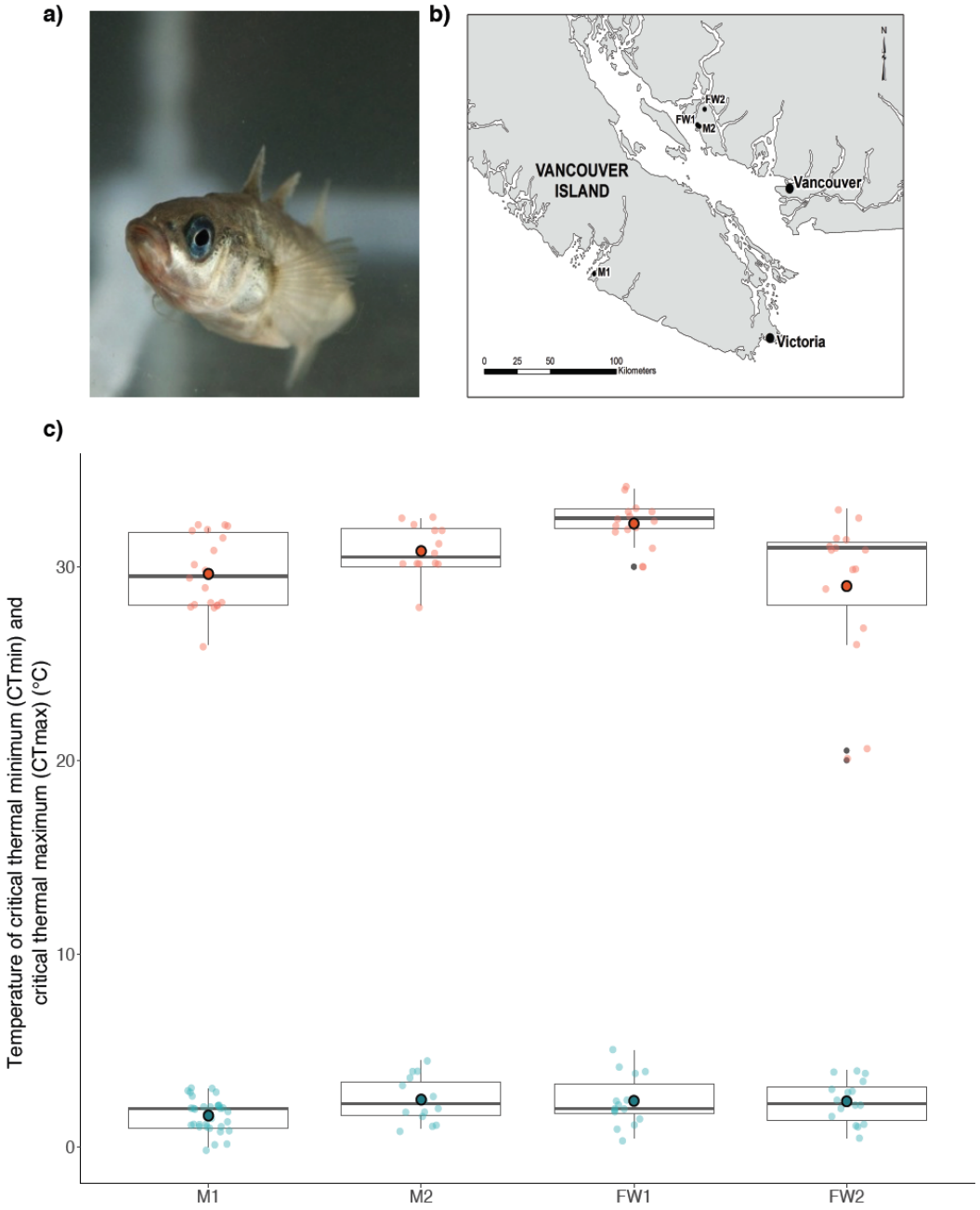

Figure 1. a) Adult threespine stickleback (*Gasterosteus aculeatus*) from a single genetic cluster were sampled from b) two marine and two freshwater populations in the Canadian Pacific Northwest. These populations were assayed for c) critical thermal minima and maxima. Thermal trait values for marine populations (M1 and M2) were incorporated into the species distribution models, while marine and freshwater populations (M1, FW1, and FW2) were used to generate F1 and F2 generations for linkage map construction and quantitative trait loci (QTL) analyses.

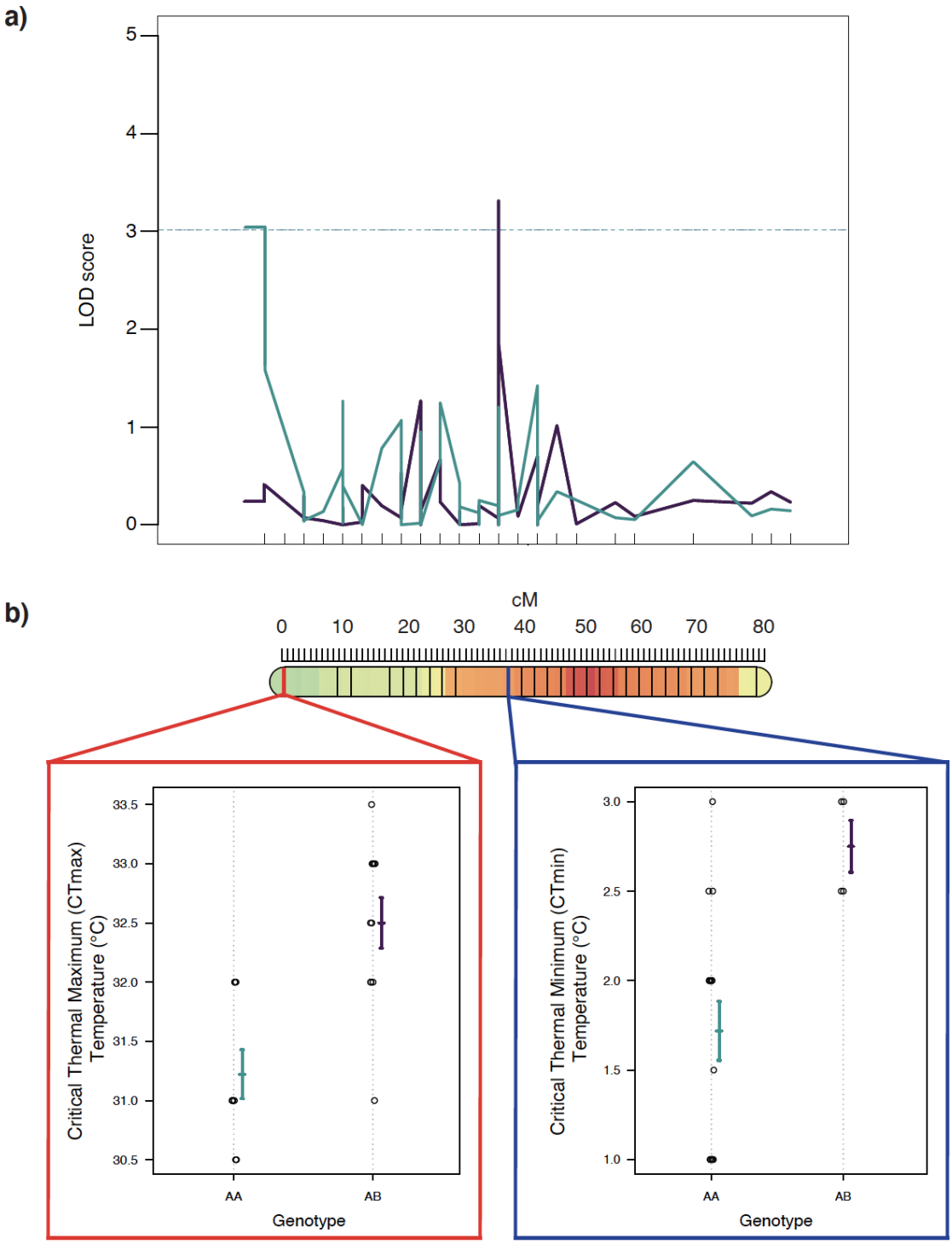

Figure 2. a) Quantitative trait loci (QTL) scan of linkage group 4 with trait-specific significance thresholds for LOD scores, showing a significant LOD peak for CTmin (dark purple) and CTmax (light blue) with b) an inset of linkage group 4 highlighting the position of the significant QTL for upper and lower thermal tolerances (CTmax and CTmin, respectively).

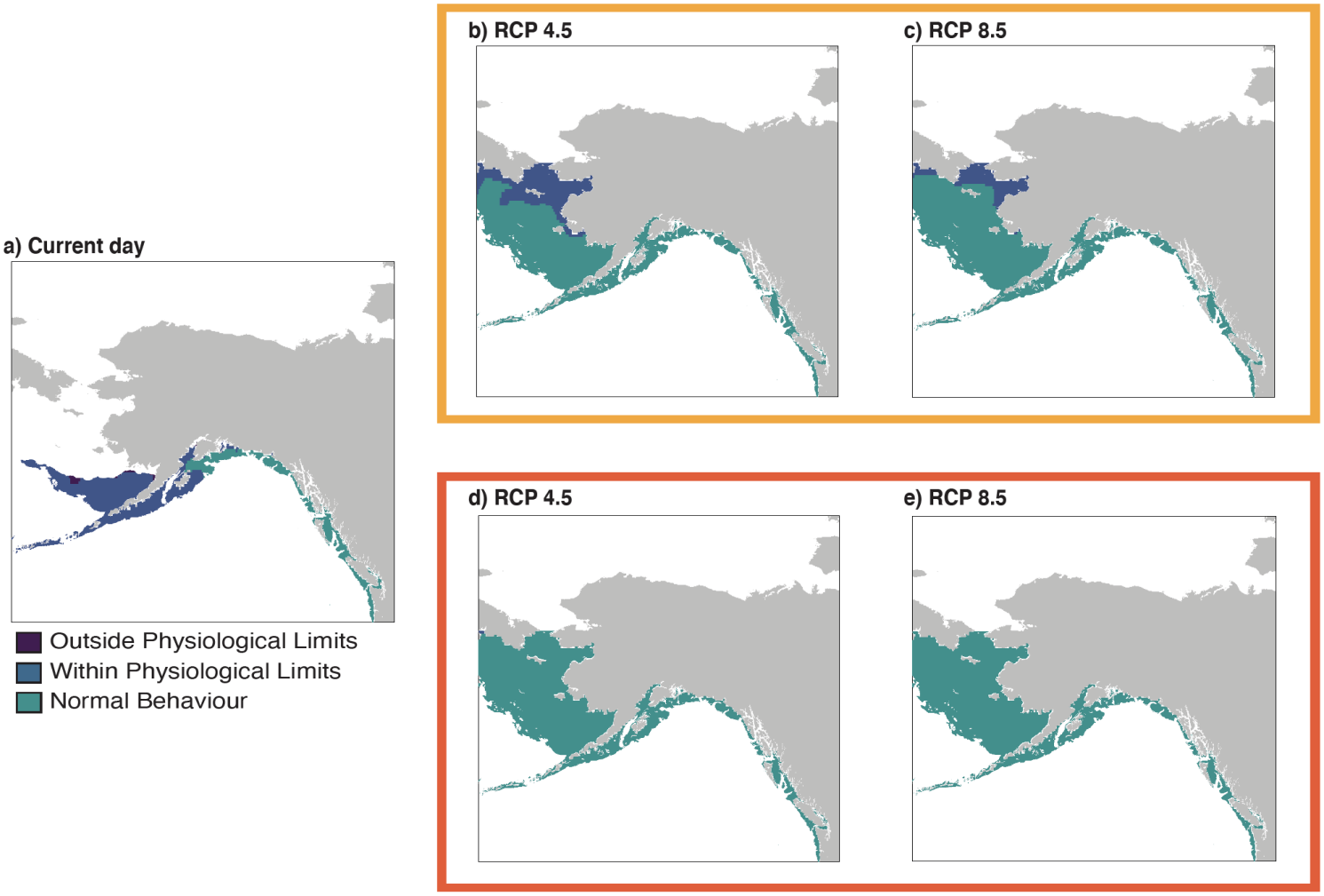

Figure 3. Changes in the distribution of marine threespine stickleback (*Gasterosteus aculeatus*) as a result of incorporating thermal traits in a) current day environmental conditions and under IPCC end-of-century projections RCP 4.5 and 8.5 without trait evolution ('no evolution' model, b & c, orange box) and with trait evolution ('evolution' model, d & e, red box)**.**

Supplementary Figures and Tables

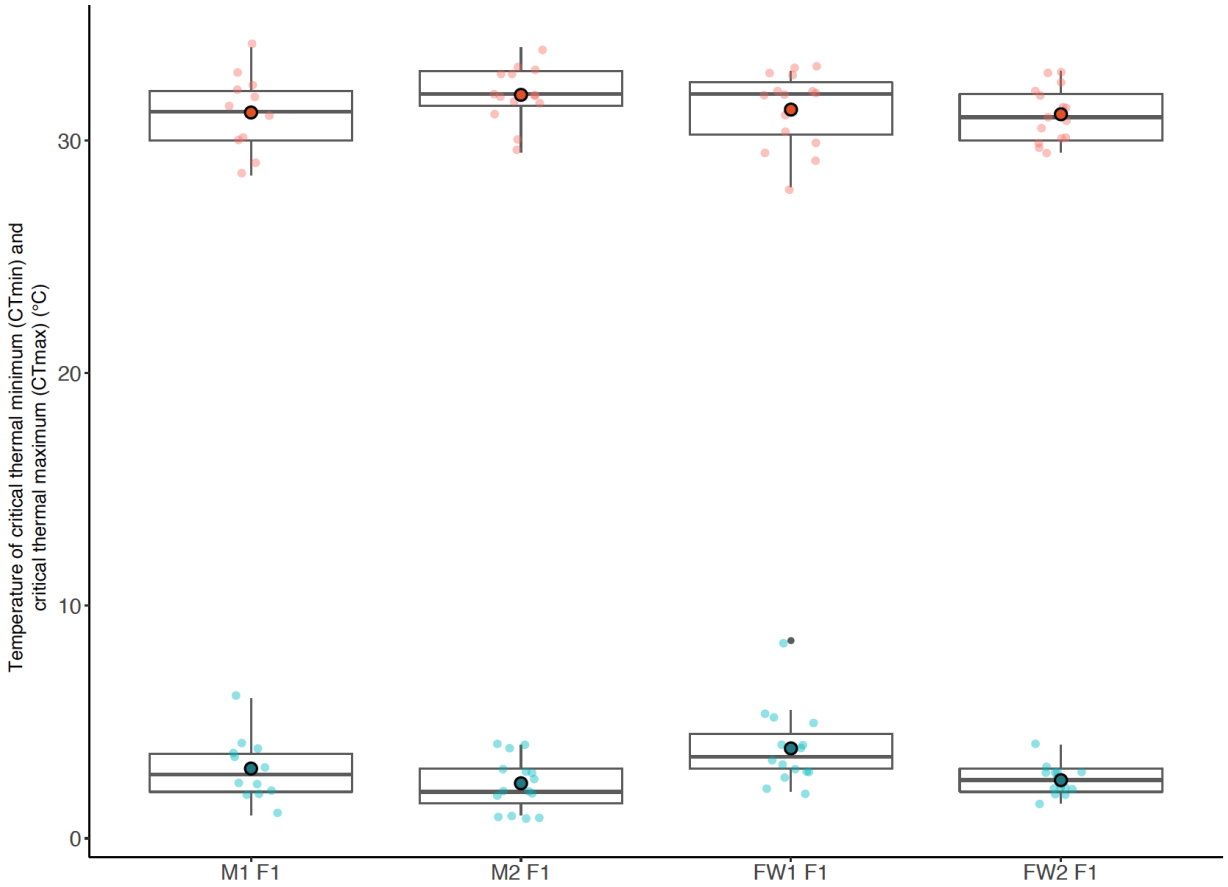

Figure S1. Critical thermal minimum (CTmin) and maximum (CTmax) measurements for adult threespine stickleback (*Gasterosteus aculeatus*) from pure F1 marine (M*F1) and freshwater (FW*F1) families raised in a common garden under a constant thermal environment.

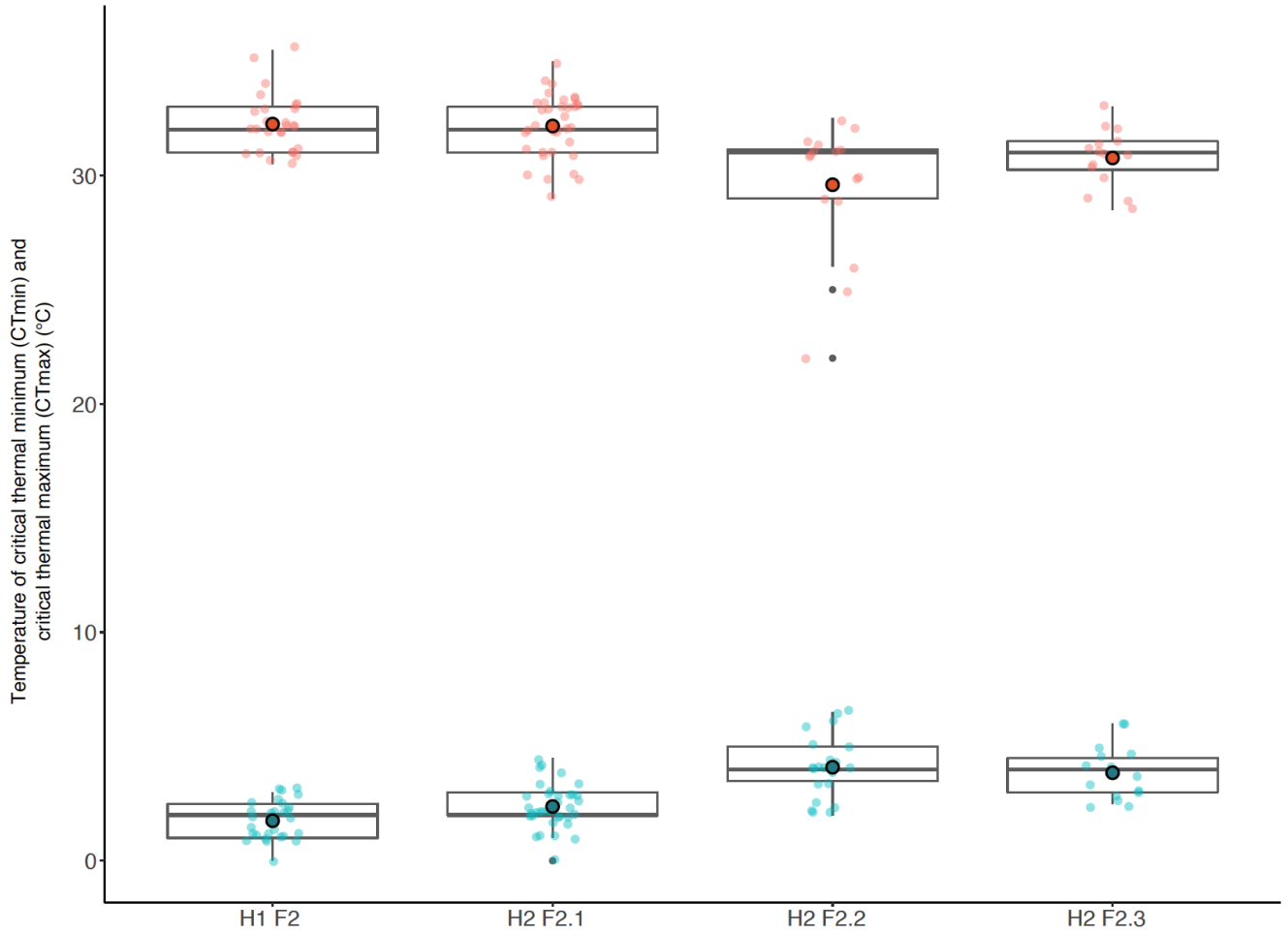

Figure S2. Critical thermal minimum (CTmin) and maximum (CTmax) measurements for adult threespine stickleback (*Gasterosteus aculeatus*) from hybrid marine-freshwater F2 families raised in a common garden under a constant thermal environment.

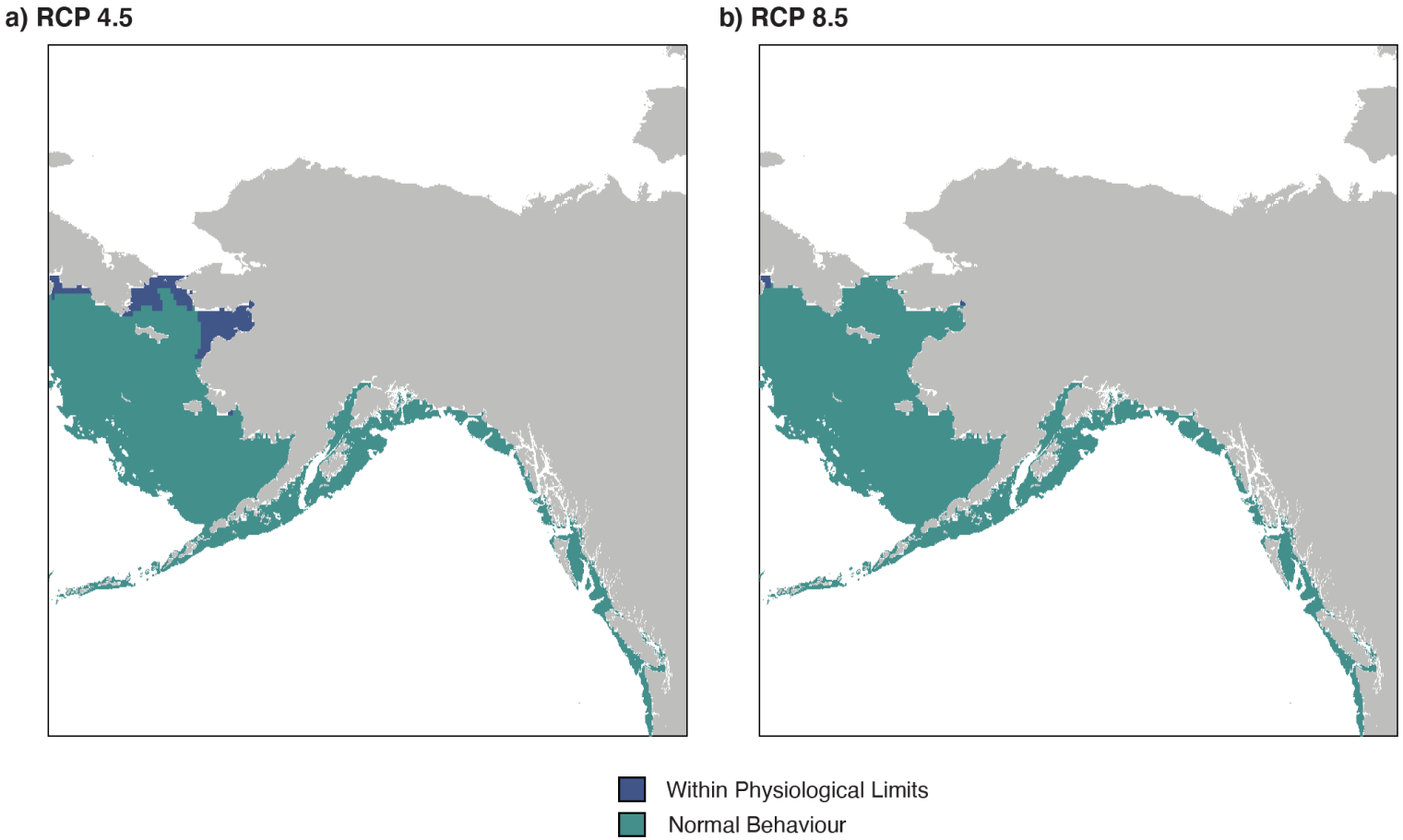

Figure S3. Changes in the distribution of marine threespine stickleback (*Gasterosteus aculeatus*) as a result of incorporating thermal traits under IPCC end-of-century projections RCP 4.5 and 8.5 with trait evolution constrained by the underlying genetic architecture of critical thermal minimum (CTmin) as determined from hybrid F2 mapping families.

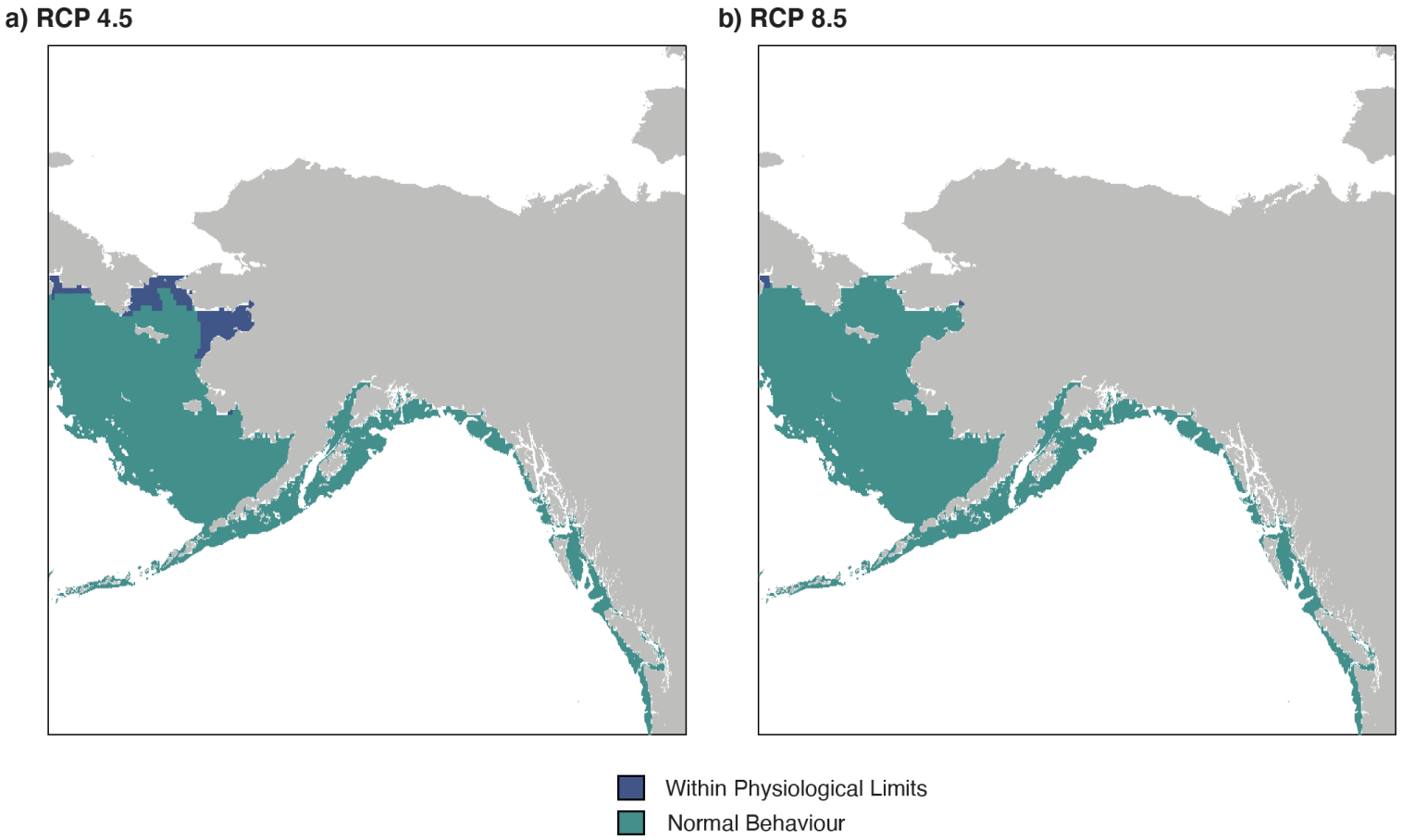

Figure S4. Changes in the distribution of marine threespine stickleback (*Gasterosteus aculeatus*) as a result of incorporating thermal traits under IPCC end-of-century projections RCP 4.5 and 8.5 with trait evolution constrained by the underlying genetic architecture of critical thermal minimum (CTmin) and critical thermal maximum (CTmax) as determined from hybrid F2 mapping families.

Table S1. Summaries of family-specific linkage maps constructed for quantitative trait loci (QTL) analyses.

Map	$n_{markers}$	**Length (cM)**	**Avg. Max. Spacing**
KL1	2139	1370.4	7.6
KL2	1558	1311	8.5
KL3	1964	1359.5	7.9
HL	5247	1621.1	11.8

Table S2. Thermal trait data from *Gasterosteus aculeatus* used to inform the species distribution envelopes (rows) in the varied evolutionary scenarios (columns) projected for end-of-century conditions.

	Current day	No evolution	Adjusted PVE	Evolution
Normal Behaviour	(5 - 25)	(5 - 25)	(3.6 - 25)	(2.5 - 25)
Within Physiological Limits	(0.9 - 31.9)	(0.9 - 31.9)	(0 - 31.9)	(0 - 31.9)
Outside Physiological Limits	$31.9 > x < 0.9$	$31.9 > x < 0.9$	$31.9 > x < 0$	$31.9 > x < 0$